Wang, Qiqin et al., 2014. Enantioseparation of N-derivatized amino acids by micro-liquid chromatography using carbamoylated quinidine functionalized monolithic stationary phase. Journal of Chromatography A, 1363, pp.207–215.

Title: Enantioseparation of *N*-derivatized amino acids by micro-liquid chromatography using carbamoylated quinidine functionalized monolithic stationary phase

Author: Qiqin Wang Jun Feng Hai Han Peijie Zhu Huihui Wu María Luisa Marina Jacques Crommen Zhengjing Jiang

PII: S0021-9673(14)00963-7
DOI: http://dx.doi.org/doi:10.1016/j.chroma.2014.06.039
Reference: CHROMA 355518

To appear in: *Journal of Chromatography A*

Received date: 14-4-2014
Revised date: 12-6-2014
Accepted date: 12-6-2014

Please cite this article as: Q. Wang, J. Feng, H. Han, P. Zhu, H. Wu, M.L. Marina, J. Crommen, Z. Jiang, Enantioseparation of *N*-derivatized amino acids by micro-liquid chromatography using carbamoylated quinidine functionalized monolithic stationary phase, *Journal of Chromatography A* (2014), http://dx.doi.org/10.1016/j.chroma.2014.06.039

Enantioseparation of *N*-derivatized amino acids by micro-liquid chromatography using carbamoylated quinidine functionalized monolithic stationary phase

Qiqin Wang[1,2#], Jun Feng[1#], Hai Han[1], Peijie Zhu[1], Huihui Wu[1], María Luisa Marina[2], Jacques Crommen[1,3], Zhengjing Jiang[1,*]

[1]*Department of Pharmacy and Guangdong Province Key Laboratory of Pharmacodynamic Constituents of Traditional Chinese Medicine & New Drug Research, Jinan University, Guangzhou 510632, China*

[2] *Department of Analytical Chemistry, Physical Chemistry and Chemical Engineering, Faculty of Biology, Environmental Sciences and Chemistry, University of Alcalá, Ctra. Madrid-Barcelona, Km. 33.600, 28871 Alcalá de Henares (Madrid), Spain*

[3]*Laboratory of Analytical Pharmaceutical Chemistry, Department of Pharmaceutical Sciences, University of Liege, CHU B36, B-4000 Liege, Belgium*

[*]*Corresponding author*

Tel.:+86 2085223604

E-mail address: jzjjackson@hotmail.com

[#] *These authors contributed equally to this work.*

Abstract:

In order to obtain satisfactory column permeability, efficiency and selectivity for micro-HPLC, a capillary monolithic column containing *O*-9-[2-(methacryloyloxy)-ethylcarbamoyl]-10,11-dihydroquinidine (MQD) as chiral selector was re-optimized. The monolithic column was used to successfully enantioresolve a wide range of *N*-derivatized amino acids including alanine, leucine, methionine, threonine, phenylalanine, valine, serine, isoleucine, tryptophan, and cysteine. The influence of mobile phase parameters, such as the organic solvent type and concentration, the apparent pH, and buffer concentration, on retention and enantioseparation of *N*-derivatized amino acids has been investigated. 3,5-dinitrobenzoyl-amino acids and 3,5-dichlorobenzoyl-amino acids were resolved into enantiomers with exceptionally high selectivity and resolution. The chemoselectivity of the monolithic column for a multicomponent mixture of *N*-derivatized amino acids was also investigated. A mixture of three pairs of 3,5-dichlorobenzoyl-amino acids could be fully resolved in 22.5 minutes.

Keywords: carbamoylated quinidine / enantioseparations / *N*-derivatized amino acids / monolithic columns / micro-HPLC

1. Introduction

The stereochemistry of amino acids plays an important role in their biological and pharmacological properties. An increasing number of observations suggests that $_{D}$-amino acids have a significant influence in living organisms, including humans [1]. Some $_{D}$-amino acids have been found to be related to different diseases, including schizophrenia [2], Alzheimer's disease [3] and renal disorders [4]. For example, $_{D}$-serine may be useful as a biomarker and even a therapeutic agent for neurological disorders [5], while $_{L}$-serine plays a key role in the central nervous system and cellular proliferation [6]. Moreover, amino acids as chiral building blocks have a significant importance for synthetic therapeutic peptides [7]. However, it is difficult to resolve free amino acids into their enantiomers because of an obvious lack of appropriate functionalities to interact with the chiral selectors [8]. In order to enhance the intermolecular interaction between amino acids and chiral selectors, additional interaction sites could be introduced through the derivatization of amino groups [9], using reagents such as carbazole-9-carbonyl (CC) chloride [9], 2,4-dinitrophenyl (DNP) fluoride [10], 4-fluoro-7-nitro-2,1,3-benzoxadiazole (NBD-F) [11], or dansyl (DNS) chloride [12]. These UV-absorbing or fluorescent derivatization agents could also bring a strong chromophore or fluorophore into amino acids and peptides for improving detection sensitivity [9,13]. Therefore, the enantioseparation of *N*-derivatized amino acids remains a hot research topic even if well advanced. A series of chiral stationary phases (CSPs), containing polysaccharides [14], macrocyclic antibiotics [15], native or cationic cyclodextrins (CD) [16], and *(S)-N*-3,5-dinitrobenzoyl-1-naphthylglycine [17] as chiral selectors, have been applied to the enantioseparation of different kinds of *N*-derivatized amino acids. In particular, carbamoylated quinine and quinidine immobilized on silica microparticles have received great attention due to their excellent enantioselectivity towards various kinds of acidic analytes, such as *N*-derivatized amino acids [18-19], profens [20], α-aryloxy alkanoic acids [18], 1,4-dihydropyridine monocarboxylic acid [21], pyrethroic acids [22], *N*-derivatized peptides [23], dafachronic acids [24], and aminophosphonic acids [25]. The enantioselectivity could be attributed to a global effect, including ion-pair formation between chiral analytes and selector, dipole-dipole, hydrophobic, hydrogen bonding, π-π and steric interactions [26].

In the last decade, monolithic columns have proved to be an effective alternative to

packed columns and have attracted considerable interest owing to their facile preparation methodology and good column characteristics, such as permeability and efficiency [27]. Lämmerhofer et al. developed quinine and quinidine-based chiral monolithic columns, namely poly (O-9-(*tert*-butylcarbamoyl)-11-[2-(methacryloyloxy)ethylthio] -10,11-dihydroquinine-*co*-2-hydroxyethyl methacrylate-*co*-ethylene dimethacrylate) and poly (O-9-[2-(methacryloyloxy)-ethylcarbamoyl]-10,11-dihydroquinidine-*co*-2-hydroxyethyl methacrylate-*co*-ethylene dimethacrylate) (poly(MQD-*co*-HEMA-*co*-EDMA)) for capillary electrochromatography (CEC) applications by *in situ* copolymerization of O-9-(*tert*-butylcarbamoyl)-11-[2-(methacryloyloxy)ethylthio]-10,11-dihydroquinine or O-9-[2-(methacryloyloxy)-ethylcarbamoyl]- 10,11-dihydroquinidine [12,28]. These macroporous chiral monolithic columns exhibited very good enantioselectivity and column efficiency in the CEC mode for several *N*-derivatized amino acids, such as CC-Alanine, CC-Serine, and 3,5-dinitrobenzoyl (DNB)-Leucine [12,28-30]. However, their applicability to micro-HPLC separations does not seem to have been investigated so far. It is well known that the column properties required for micro-HPLC are different from those for CEC. Therefore, a systematic optimization of the polymerization conditions is required in order to obtain satisfactory micro-HPLC performance with respect to column permeability, mechanical stability, efficiency and selectivity. Besides, it is of high interest to systematically evaluate the enantioselectivity of poly(MQD-*co*-HEMA-*co*-EDMA) monolithic columns towards a wider range of analytes since only a few derivatives of leucine and valine have been examined so far [12,28-30].

In this study, a capillary liquid chromatography column containing carbamoylated quinidine was prepared according to Lämmerhofer et al [28]. In order to obtain satisfactory column permeability, efficiency and selectivity in micro-HPLC, the composition of the polymerization mixture was re-optimized. The optimized monolithic column was subsequently applied to the enantioseparation of various kinds of *N*-derivatized amino acids, containing benzoyl (B), *p*-nitrobenzoyl (*p*-NB), 3,5-dinitrobenzoyl (3,5-DNB), 3,5-dimethoxybenzoyl (3,5-DMB), 9-fluorenylmethoxycarbonyl (Fmoc), 3,5-dichlorobenzoyl (3,5-DClB), *m*-chlorobenzoyl (*m*-ClB), *p*-chlorobenzoyl (*p*-ClB), or *o*-chlorobenzoyl (*o*-ClB) protecting groups. The influence of the organic solvent type and content, the buffer

concentration and the apparent pH of the mobile phase on the enantioseparation of these amino acid derivatives has also been investigated. The separation mechanism is also discussed on the basis of a comparison of the influence of the type of *N*-protecting group and amino acid on enantioseparation.

2. Experimental

2.1. Chemicals and materials

3-(Trimethoxysilyl)-propyl methacrylate (γ-MAPS), 2,2'-azobisisobutyronitrile (AIBN), 2-hydroxyethyl methacrylate (HEMA), ethylene dimethacrylate (EDMA), methanol (MeOH), dodecanol, chloroform, cyclohexanol, acetonitrile (ACN), acetic acid, ammonium formate , ammonium acetate and dibutyltin dilaurate were all purchased from Aladdin Chemicals (Shanghai, China). 4-Methoxyphenol and 2-isocyanatoethyl methacrylate were obtained from Maya Reagent (Jiaxing, Zhejiang, China). All racemic amino acids (alanine, leucine, methionine, threonine, phenylalanine, valine, serine, isoleucine, tryptophan, and cysteine), 10,11-dihydroquinidine (DHQD) and nine aroyl chlorides (*p*-nitrobenzoyl chloride, 3,5-dinitrobenzoyl chloride, 3,5-dimethoxybenzoyl chloride, 9-fluorenylmethoxycarbonyl chloride, 3,5-dichlorobenzoyl chloride, *m*-chlorobenzoyl chloride, *p*-chlorobenzoyl chloride, benzoyl chloride, and *o*-chlorobenzoyl chloride) were purchased from Energy Chemical (Shanghai, China). All *N*-derivatized amino acids were synthesized according to a standard procedure [31] except Fmoc and 3,5-DClB derivatives. As described previously [32], amino acids were amidated by 9-fluorenylmethoxycarbonyl chloride in aqueous solution to afford Fmoc-derivatized amino acids. 3,5-DClB derivatives were synthesized through reaction of amino acids with 3,5-dichlorobenzoyl chloride in THF [33]. Distilled water was filtered through a 2-μm membrane before use. The fused-silica capillaries (375 μm O.D. × 100 μm I.D.) were obtained from Ruifeng Chromatography Ltd. (Yongnian, Hebei, China).

2.2. Instrumentation

All scanning electron microscopy (SEM) experiments were carried out using an ultra-high 165 resolution Hitachi S-4800 SEM (Tokyo, Japan) at an acceleration voltage of 1 kV. A Jinghong DK-S22 water bath (Shanghai, China) was used for thermally initiated copolymerization. All micro-HPLC experiments were carried out

on a self-assembled HPLC system that consisted of a DiNa nano gradient pump (Tokyo, Japan), a Valco four-port injection valve with 20 nL internal loop (Houston, TX, USA), and a Shimadzu SPD-15C UV detector (Kyoto, Japan). Data acquisition and data handling were performed using a Unimicro Trisep^{TM} Workstation 2003 (Shanghai, China). All chromatograms were converted to a text file and redrawn using Microcal Origin 8.0. The pH values were monitored by a Sartorius PB-10 pH meter (Gottingen, Germany).

2.3. Chromatographic conditions

Unless otherwise stated, the mobile phase was a mixture of ACN/0.1 M ammonium acetate (80/20; v/v). The mobile phase apparent pH was adjusted to the desired value by adding acetic acid. All chiral samples were dissolved in MeOH to reach a final concentration around 1 mg/mL. The mobile phase was filtered through a 0.22-μm membrane and degassed before use. The flow rate of the mobile phase was set at 1 μL/min and the injection volume was 20 nL. The analytes were all detected at a wavelength of 254 nm.

2.4. Preparation of poly(MQD-*co*-HEMA-*co*-EDMA) monolithic columns

2.4.1. Synthesis of *O*-[2-(Methacryloyloxy)ethylcarbamoyl]-10,11-dihydroquinidine

The functional monomer MQD was synthesized according to Lämmerhofer et al. [28] using a properly modified procedure. In brief, 2-isocyanatoethyl methacrylate (1.4 mL, 10 mmol) was added to a mixture of DHQD (1.3 g, 4 mmol), dibutyltin dilaurate (10 drops) and 4-methoxyphenol (10 mg) in THF (30 mL), followed by stirring for 96 h at room temperature. The mixture was filtered, concentrated under reduced pressure. The residue was purified on a packed silica column using a eluent consisting of chloroform /MeOH (40:1; v/v) to afford MQD (white powder, yield 58.7%).

2.4.2. Preparation of poly(MQD-*co*-HEMA-*co*-EDMA) monolithic columns

The monomers (MQD, HEMA, and EDMA), the binary porogenic mixture (1-dodecanol and cyclohexanol) and the initiator AIBN (1 wt% with respect to the monomers) were mixed ultrasonically into a homogenous solution in a 2-mL vial. The composition of the polymerization mixture was optimized in order to obtain

satisfactory permeability and selectivity (**Table 1**). After sonication and bubbling with nitrogen for 5 min, this polymerization mixture was transferred into a 20-cm long capillary, which had been pretreated with γ-MAPS in order to afford anchoring sites for the polymeric bulk [34-35]. The filled capillaries were sealed with GC septa and submerged into a water bath at 60 ^{o}C for 20 h. The obtained monolithic columns were then flushed out using MeOH in order to remove unreacted chemicals and porogens. A 2-3 mm detection window was created at a distance of 3 cm from the end of the column using a thermal wire stripper. The capillary column was cut into a total length of 18 cm with an effective length of 15 cm. The finally obtained bulk polymer was taken for elemental analysis. A 3-5 mm length of monolith was then cut, placed on an aluminum stub and then sputter-coated with gold for SEM analysis.

2.5. Calculations

The enantioselectivity (α) was calculated according to the following expression: $\alpha = k_2/k_1$ where $k = (t_R\text{-}t_0)/t_0$ (t_0 is the elution time of the solvent peak, which was used as the dead time, t_{R1}, t_{R2}, k_1 and k_2 are the retention times and the retention factors of the first and second eluting enantiomers, respectively) [34]. The theoretical plate number (N) and the resolution factor (R_s) were determined according to the standard equations based on their corresponding widths at half-height [36].

3. Results and discussion

3.1. Preparation and optimization of poly(MQD-*co*-HEMA-*co*-EDMA) monolithic columns

Lämmerhofer et al. previously prepared successfully a quinidine-based chiral monolithic column for enantioseparations in the CEC mode [28]. However, a column with satisfactory performance in CEC might not be suitable for a successful HPLC separation. The permeability is a very important property of an HPLC column because of its direct and indirect influence on a number of factors, such as stability, analysis time, column efficiency, resolution etc. In order to obtain a poly (MQD-*co*-HEMA-*co*-EDMA) monolithic column with satisfactory permeability and efficiency in micro-HPLC, the composition of the polymerizable mixture was re-optimized as shown in **Table 1** by evaluating the properties and structure of the monoliths using micro-HPLC and SEM.

In order to investigate the effect of the porogens in the reaction mixture, the weight content of the binary porogenic mixture was varied from 70% (C1) to 60% w/w (C3) while the composition of monomers and porogens was kept constant. It was observed that the decrease of the total weight content of porogens resulted in a clear increase of the backpressure from 2.9 MPa to 10.1 MPa. Column C2 exhibited a suitable backpressure and the highest column efficiency (24400 theoretical plates/m at a linear flow rate of 1.1 mm/s using naphthalene as test compound) when compared to columns C1 and C3.

It was also observed that the co-monomer HEMA affected the column performance. As the weight fraction of HEMA in the monomers increased from 52.5% (C2) to 57.5% (C5) w/w, the theoretical plate number increased from 24400 to 32000 plates/m while the backpressure remained almost constant. A further increase of the HEMA weight content to 60% (C6) caused a significant increase of backpressure and a slight decrease in column efficiency. Therefore, considering the column permeability and efficiency, a HEMA weight content of 57.5% in the monomers was selected for all further experiments.

The composition of the porogenic mixture (dodecanol/cyclohexane ratio) was also taken into consideration. The micro-HPLC experiments showed that the column backpressure increased from 5.8 MPa to 13.1 MPa when the content of dodecanol decreased from 88.33% (C7) to 78.33% (C8) wt%. On the other hand, the best column efficiency was obtained on column C5 with 83.33 % dodecanol in the porogenic mixture.

Finally, a polymerization mixture consisting of 35 wt% monomers (MQD/HEMA/EDMA, 20/57.5/22.5, w/w/w) and 65 wt% porogens (dodecanol/cyclohexanol, 83.33/16.67, w/w) was chosen for all further studies since it yielded the monolith C5 exhibiting uniform structure and good permeability and efficiency. **Fig. 1a** and **Fig. 1b** shows the SEM result for column C5, where spherical units agglomerate into large clusters interdispersed by large-pore channels.

3.2. Permeability and reproducibility of poly(MQD-*co*-HEMA-*co*-EDMA) monolithic columns

The permeability of the poly(MQD-*co*-HEMA-*co*-EDMA) monolithic column was determined by pumping ACN, MeOH, and water through it at different linear flow rates. According to Bristow and Knox [37], the permeability K can be expressed as

follows:

$$K = (uL/\Delta P)\eta$$

where η is the dynamic viscosity of the eluent, u is the linear velocity of the mobile phase, L is the length of the column, and ΔP is the pressure drop across the column. Since toluene was unretained in organic mobile phases, it was selected as dead-time marker when ACN and MeOH were used as eluents. When using water as mobile phase, thiourea was selected as t_0 marker. The good mechanical stability of column C5 could be evidenced by the excellent linearity between backpressure and linear velocity over the pressure range of 0-13 MPa (Figure not shown). The calculated K values for column C5 are given in **Table 2**. The results indicate a high permeability for the optimized poly(MQD-*co*-HEMA-*co*-EDMA) monolithic column, which is ideal for HPLC applications.

In addition, the reproducibility of the poly(MQD-*co*-HEMA-*co*-EDMA) monolithic columns was assessed by determining the relative standard deviations (RSDs) for the retention factors of two test analytes, i.e. anisole and naphthalene. A mixture of ACN/H_2O (40/60, v/v) was used as mobile phase. The RSD values for run to run (n = 10) repeatability of anisole and naphthalene retention factors were 0.88% and 1.08%, respectively. The RSD values for day to day (n=5) repeatability were 2.18% and 2.78%, respectively. These data demonstrate the stability of the poly(MQD-*co*-HEMA-*co*-EDMA) monolithic columns, since their properties do not seem to change significantly either with time or with the number of injections. Furthermore, the batch to batch (n=3) reproducibility values for anisole and naphthalene retention factors were 4.38% and 4.47%, respectively. These results further confirm the good reproducibility of the optimized poly(MQD-*co*-HEMA-*co*-EDMA) monolithic columns.

3.3. Effects of mobile phase composition on enantioseparation

In order to systematically evaluate the enantioselectivity of the optimized poly(MQD-*co*-HEMA-*co*-EDMA) monolithic columns in the micro-HPLC mode, two *N*-derivatized amino acids, i.e. 3,5-DNB-Leucine and 3,5-DClB-Leucine, were chosen as test analytes. The influence of the organic solvent type and concentration, the apparent pH and the buffer concentration was investigated.

The influence of the organic solvent type (MeOH and ACN) in the mobile phase on retention times and enantioselectivity was first studied. Both 3,5-DNB-Leucine and

3,5-DClB-Leucine could be enantioseparated with mixtures of either MeOH/0.1 M ammonium acetate (80/20, v/v, apparent pH = 5.3) or ACN/0.1 M ammonium acetate (80/20, v/v, apparent pH = 5.3) as mobile phase. However, the retention of the second enantiomer of 3,5-DNB-Leucine was too high to be eluted from the column within 120 min when MeOH/0.1 M ammonium acetate (80/20, v/v, apparent pH = 5.3) was used as mobile phase. Therefore ACN/H_2O system was chosen for studying the influence of the organic solvent concentration on the enantioseparation of the two *N*-derivatized amino acids. As can be seen in **Table 3**, the retention factors of both analytes increased dramatically with decreasing ACN content from 80 to 60%. However the enantioselectivity (α) remained fairly constant over the studied ACN concentration range while the enantioresolution (R_s) increased with decreasing ACN concentration, owing to increasing retention and column efficiency. This might suggest that part of the retention on the poly(MQD-*co*-HEMA-*co*-EDMA) monolithic stationary phase under the tested conditions is due to hydrophobic interaction and that the latter is not responsible for enantioselectivity. In order to find the best compromise between retention times and enantioresolution, a mobile phase containing 80% ACN was considered as the most suitable for further experiments.

It has been reported that the electrostatic interactions between the negatively charged carboxylate function of *N*-derivatized amino acids and the positively charged tertiary nitrogen of quinidine play an important role in the enantioselectivity of quinidine-based stationary phases [8]. The mobile phase pH could affect the ionization state of both quinidine (pKa = 8.72) [38] stationary phase and analytes, i.e. 3,5-DNB-Leucine (pKa = 3.77) [39] and 3,5-DClB-Leucine (pKa = 3.79) [39]. Therefore its effect on the enantioseparation of the two *N*-derivatized amino acids was also investigated by adjusting the apparent pH value of the mobile phase (ACN/0.1 M ammonium acetate (80/20; v/v)) to 6.3, 5.3 and 4.3 after mixing with ACN. As shown in **Table 4**, both retention factors (k_1 and k_2) and R_s of 3,5-DNB-Leucine and 3,5-DClB-Leucine decreased with decreasing mobile phase apparent pH from 6.3 to 4.3. The α values remained almost constant between pH 6.3 and 5.3, and then decreased significantly at pH 4.3. This behavior is certainly related to the fact that in the selected apparent pH range, the quinidine stationary phase remains fully positively charged while the negative charge of the two *N*-derivatized amino acids will start decreasing with decreasing apparent pH, resulting in a reduction of electrostatic

interactions and hence of enantioselectivity. Finally, an apparent pH of 5.3 was selected because it represented the best compromise between enantioresolution and analysis time.

The influence of the buffer concentration was also investigated by varying the concentration of ammonium acetate from 0.05 to 0.15 M, while the other chromatographic conditions were kept constant (**Table 5**). No significant influence on enantioselectivity for both *N*-derivatized amino acids was observed in this concentration range. However, their retention and enantioresolution clearly increased with decreasing ammonium acetate concentration. These results might indicate that the contribution of electrostatic interactions to the retention of these acidic analytes increases with decreasing concentration of the competing anion acetate. A 0.1 M concentration of ammonium acetate was found to be the most suitable with respect to enantioresolution and analysis time.

3.4. Enantioseparation of *N*-derivatized amino acids

In order to systematically evaluate the enantioselectivity of poly (MQD-*co*-HEMA-*co*-EDMA) monolithic columns in the micro-HPLC mode, various kinds of *N*-derivatized amino acids were synthesized and enantioseparated (**Table 6**). The tagging reagents used to derivatize the amino acids included the following *N*-protecting groups: B, *p*-NB, 3,5-DNB, 3,5-DMB, Fmoc, 3,5-DClB, *m*-ClB, *p*-ClB and *o*-ClB (**Fig. 2**).

The results (k_1, k_2, α, R_s, N_1 and N_2) obtained for 47 *N*-derivatized amino acids (alanine, isoleucine, leucine, methionine, valine, threonine, phenylalanine, cysteine, serine, and tryptophan derivatives) on poly (MQD-*co*-HEMA-*co*-EDMA) monolithic columns are given in **Table 6**. Under the selected chromatographic conditions, 44 out of 47 analytes could be baseline enantioresolved ($R_s > 1.5$), and the other three analytes could be partially enantioseparated ($0.74 \leq R_s < 1.5$). The highest enantioresolution values were observed for 3,5-DNB derivatives, followed by 3,5-DClB derivatives. It was also noticed that the poly (MQD-*co*-HEMA-*co*-EDMA) monolithic column optimized for micro-HPLC could offer a better enantioselectivity within a shorter analysis time comparing with the previously reported poly (MQD-*co*-HEMA-*co*-EDMA) monolithic column used in CEC [28]. For instance, α value of ~ 2.91 and R_s value of ~ 8.44 for 3,5-DNB-Leucine enantiomers were obtained over 40 minutes in the CEC mode [28], while α value of ~ 4.71 and R_s value

of ~ 8.51 for 3,5-DNB-Leucine enantiomers were reached less than 12 minutes in the micro-HPLC mode. These results further demonstrate the great potential of the poly(MQD-*co*-HEMA-*co*-EDMA) monolithic column to enantioresolve a wide range of *N*-derivatized amino acids.

When the results in **Table 6** are more closely examined, a similar trend in enantioselectivity for amino acid derivatives in each series was noticed. For instance, α values for 3,5-DClB amino acid enantiomers were in the following rank order: isoleucine > valine > phenylalanine > leucine > tryptophan > methionine > threonine > cysteine > alanine > serine. Lindner et. al. showed that the lipophilicity and bulkiness of the side chain of the analytes may affect the enantiodiscrimination potential of quinidine-based columns [8]. Furthermore, they found that an increase of the size and bulkiness of the side chain leads to an enhancement in the retention of the second eluting enantiomer [8]. Interestingly, a similar phenomenon was observed in this study. For instance, the α-values for some aliphatic amino acid enantiomers as 3,5-DClB derivatives increase in the order: serine (hydroxymethyl, α = 2.18) < cysteine (thiomethyl, α = 2.28) < threonine (1-hydroxyethyl, α = 2.57), and alanine (methyl, α = 2.21) < leucine (isobutyl, α = 3.12) < isoleucine (*sec*.-butyl, α = 4.24).

In order to study the influence of *N*-protecting groups on the enantioseparation, eight different *N*-derivatized leucine derivatives were selected. As shown in **Table 7** and **Fig. 3**, baseline enantioseparation could be achieved on the poly (MQD-*co*-HEMA-*co*-EDMA) column for all eight analytes. Furthermore, the enantioselectivity for the amino acid derivatives decreased with decreasing electrophilic character of the *N*-protecting groups. This trend could be deduced from the reduction of enantioselectivity obtained by exchanging the strong π-acidic 3,5-DNB groups for the weaker π-acidic *p*-NB and B groups: e.g. α (3,5-DNB-Leucine) = 4.71 > α (*p*-NB-Leucine) = 1.74 > α (B-Leucine) = 1.34. Lindner et. al. showed that the *N*-protecting groups could provide a strongly electron-deficient aromatic system for π-π interaction with the quinoline ring of quinidine [8]. The effective π-π interaction increment of the *N*-protecting groups could improve the enantioselectivity for *N*-derivatized amino acids [8].

In order to confirm the enantiomer elution order, L-form enantio-enriched 3,5-DNB-Methionine and 3,5-DNB-Alanine were used as analytes. As can be seen in **Fig. 4**, the L-enantiomers were always eluted first. The same enantiomer elution order has been previously observed for 3,5-DNB-Leucine [28] and Fmoc-Leucine [29],

which suggests that the L-enantiomers are more or less excluded from the "binding groove" of the quinidine moiety whereas the D-enantiomers better match the binding sites [8].

3.4.1. Chemoselectivity of the poly (MQD-*co*-HEMA-*co*-EDMA) monolithic column

A major limitation of CSPs is often their intrinsically limited chemoselectivity. In order to evaluate the chemoselectivity of poly(MQD-*co*-HEMA-*co*-EDMA) monolithic stationary phases, a mixture of 3,5-DClB-Leucine, 3,5-DClB-Valine, and 3,5-DClB-Tryptophan enantiomers was tested under isocratic conditions in micro-HPLC. **Fig. 5** shows that all three pairs of 3,5-DClB amino acid enantiomers could be completely separated in less than 22.5 minutes. Hence, the poly (MQD-*co*-HEMA-*co*-EDMA) monolithic column can be used for the enantioseparation of a multicomponent mixture of *N*-derivatized amino acids in the micro-HPLC mode.

4. Conclusion

In this research, a capillary monolithic column containing carbamoylated quinidine as chiral selector was re-optimized in order to obtain satisfactory column permeability, efficiency and selectivity in micro-HPLC. The optimized poly (MQD-*co*-HEMA-*co*-EDMA) monolithic column showed excellent morphology, good permeability, reproducibility, mechanical and chemical stability and satisfactory chromatographic performance in micro-HPLC. The influence of the organic solvent content, the buffer concentration and the apparent pH of the mobile phase on the retention and enantioseparation of *N*-derivatized amino acids seems to confirm that both hydrophobic and electrostatic interactions are responsible for the retention of these acidic analytes, while only the latter contribute to enantioselectivity. Based on a comparison of the influence of the type of *N*-protecting groups and amino acids on enantioseparation, it was deduced that the size and bulkiness of the side chain of amino acids as well as the electrophilic character of the *N*-protecting groups are likely to affect the enantiodiscrimination potential of the poly(MQD-*co*-HEMA-*co*-EDMA)

monolithic column. The optimized monolithic column was finally applied to the enantioseparation of a wide range of *N*-derivatized amino acids with exceptionally high selectivity values and good resolution, especially for 3,5-DNB-amino acids and 3,5-DClB-amino acids. Good chemoselectivity of the monolithic column for a multicomponent mixture of *N*-derivatized amino acids was also observed.

5. Acknowledgements

We gratefully appreciate the financial support from the National Natural Science Foundation of China (Grants: 81273477 and 8120249) and the Science and Technology Innovation Project of Guangdong Provincial Education Department (Grant: 34312014).

6. References

[1] K. Hamase, A. Morikawa, K. Zaitsu, J. Chromatogr. B 781 (2002) 73.

[2] S. Kato, Y. Kito, H. Hemmi, T. Yoshimura, J. Chromatogr. B 879 (2011) 3190.

[3] G. Fisher, N. Lorenzo, H. Abe, E. Fujita, W.H. Frey, C. Emory, M.M. Di Fiore, A. D'Aniello, Amino acids 15 (1998) 263.

[4] H. Brückner, M. Hausch, J. Chromatogr. 614 (1993) 7.

[5] M. Friedman, C.E. Levin, Amino acids 42 (2012) 1553.

[6] T.J. de Koning, K. Snell, M. Duran, R. Berger, B.T. Poll-The, R. Surtees, Biochem. J. 371 (2003) 653.

[7] R. Pell, S. Sić, W. Lindner, J. Chromatogr. A 1269 (2012) 287.

[8] M. Lämmerhofer, W. Lindner, J. Chromatogr. A 741 (1996) 33.

[9] C. Czerwenka, M. Lämmerhofer, W. Lindner, J. Sep. Sci. 26 (2003) 1499.

[10] C. Czerwenka, M. Lämmerhofer, W. Lindner, J. Pharmaceut. Biomed, 30 (2003) 1789.

[11] Y. Song, T. Funatsu, M. Tsunoda, J. Chromatogr. B 879 (2011) 335.

[12] M. Lämmerhofer, E. Tobler, E. Zarbl, W. Lindner, F. Svec, J.M.J. Fréchet, Electrophoresis 24 (2003) 2986.

[13] A. Péter, E. Vékes, A. Árki, D. Tourwé, W. Lindner, J. Sep. Sci. 26 (2003) 1125.

456 [14] Y. Li, C. Baek, B.W. Jo, W. Lee, Bull. Korean Chem. Soc. 26 (2005) 998.
457 [15] I. Ilisz, R. Berkecz, A. Péter, J. Sep. Sci. 29 (2006) 1305.
458 [16] X. Yao, T.T. Tan, Y. Wang, J. Chromatogr. A 1326 (2014) 80.
459 [17] M. Kato, T. Fukushima, N. Shimba, I. Shimada, Y. Kawakami, K. Lmai, Biomed.
460 Chromatogr. 15 (2001) 227.
461 [18] K.M. Kacprzak, W. Lindner, J. Sep. Sci. 34 (2011) 2391.
462 [19] H. Hettegger, M. Kohout, V. Mimini, W. Lindner, J. Chromatogr. A 1337 (2014)
463 85.
464 [20] K.H. Krawinkler, E. Gavioli, N.M. Maier, W. Lindner, Chromatographia 58(2003)
465 555.
466 [21] M. Lämmerhofer, O. Gyllenhaal, W. Lindner, J. Pharmaceut. Biomed. 35 (2004)
467 259.
468 [22] W. Bicker, M. Lämmerhofer, W. Lindner, J. Chromatogr. A 1035 (2004) 37.
469 [23] K. Gyimesi-Forrás, K. Akasaka, M. Lämmerhofer, N.M. Maier, T. Fujita, M.
470 Watanabe, N. Harada , W. Lindner, Chirality 17 (2005) S134.
471 [24] R. Sardella, A. Carotti, A. Gioiello, A. Lisanti, F. Ianni, W. Lindner, B. Natalini, J.
472 Chromatogr. A 1339 (2014) 96.
473 [25] A. F. Gargano, M. Kohout , P. Macíková, M. Lämmerhofer , W. Lindner, Anal.
474 Bioanal. Chem. 405 (2013) 8027. [26] V. Piette, M. Lämmerhofer, K. Bischoff,
475 W. Lindner, Chirality 9 (1997) 157.
476 [27] Z. Jiang, N.W. Smith, Z. Liu, J. Chromatogr. A 1218 (2011) 2350.
477 [28] M. Lämmerhofer, E.C. Peters, C. Yu, F. Svec, J.M. Fréchet, Anal. chem. 72 (2000)
478 4614.
479 [29] M. Lämmerhofer, F. Svec, J.M.J. Frechet, W. Lindner, J. Microcolumn Sep. 12
480 (2000) 597.
481 [30] M. Lämmerhofer, F. Svec, J.M. Fréchet, Anal. Chem. 72 (2000) 4623.
482 [31] B.S. Jursic, D. Neumann, Synthetic Commun. 31 (2001) 555.
483 [32] M.B. Gawande, P.S. Branco, Green Chem.13 (2011) 3355.
484 [33] W.H. Pirkle, T.C. Pochapsky, J. Am. Chem. Soc. 109 (1987) 5975.
485 [34] Q. Zhang, J. Guo, F. Wang, J. Crommen, Z. Jiang, J. Chromatogr. A 1325 (2014)

147.

[35] Z. Jiang, N.W. Smith, P.D. Ferguson, M.R. Taylor, Anal. Chem. 79 (2007) 1243.

[36] V. Piette, M. Lämmerhofer, W. Lindner, J. Crommen, J. Chromatogr. A 987 (2003) 421.

[37] P.A. Bristow, J.H. Knox, Chromatographia,10 (1977) 279.

[38] M. Lämmerhofer, P. Imming, W. Lindner, Chromatographia, 60 (2004) S13.

[39] https://scifinder.cas.org/scifinder/view/scifinder/scifinderExplore.jsf

493 **Figure captions**

494

495 **Fig. 1. Scanning electron microphotographs of column C5.**

496

497 **Fig. 2. Structures of amino acids and *N*-protecting groups.**

498

499 **Fig. 3. Enantioseparation of *N*-derivatized leucine derivatives on the**
500 **poly(MQD-*co*-HEMA-*co*-EDMA) monolithic column.** Conditions: column
501 dimensions: 150 mm × 100 μm I.D.; mobile phase: a). ACN/0.1 M ammonium acetate
502 (80/20, v/v) (apparent pH = 5.3) for all analytes except Fmoc-Leucine, b). ACN/0.1 M
503 ammonium acetate (50/50, v/v) (apparent pH = 5.3) for Fmoc-Leucine; UV detection
504 wavelength: 254 nm; flow rate: 1 μL/min; injection volume: 20 nL.

505

506 **Fig. 4. Elution order of 3,5-DNB-Methionine and 3,5-DNB-Alanine**
507 **enantiomers on the poly(MQD-*co*-HEMA-*co*-EDMA) monolithic column.**
508 Conditions: mobile phase, ACN/0.1 M ammonium acetate (80/20, v/v) (apparent pH =
509 5.3); other conditions as in **Fig. 3**.

510

511 **Fig. 5. Enantioseparation of 3,5-DClB-Leucine, 3,5-DClB-Valine and**
512 **3,5-DClB-Tryptophan.** Conditions: flow rate: 0.5 μL/min; samples:
513 3,5-DClB-Leucine (1, 4), 3,5-DClB-Valine (2, 5) and 3,5-DClB-Tryptophan (3, 6);
514 other conditions as in **Fig. 4**.

515

516 **Table 1. Composition of the polymerization mixtures used for the preparation of**
517 **poly(MQD-*co*-HEMA-*co*-EDMA) monolithic columns and their properties.**
518 Conditions: column dimensions: 150 mm × 100 μm I.D.; mobile phase, ACN/H_2O
519 (40/60, v/v); UV detection wavelength: 214 nm; flow rate: 1 μL/min; injection
520 volume: 20 nL; sample: naphthalene.

521

522

523 **Table 2. Permeability of the poly(MQD-*co*-HEMA-*co*-EDMA) monolithic column**

[a] Relative polarity data were obtained from http://virtual.yosemite.cc.ca.us/smurov/orgsoltab.htm; viscosity data of pure solvents were obtained from reference [32].

Table 3. Effect of ACN content in the mobile phase on the retention and enantioseparation of *N*-derivatized amino acids. Conditions: column: 150 mm × 100 μm I.D. poly(MQD-*co*-HEMA-*co*-EDMA); mobile phase: mixture of ACN and 0.1 M ammonium acetate at various ratios (apparent pH = 5.3); UV detection wavelength: 254 nm; flow rate: 1 μL/min; injection volume: 20 nL.

Table 4. Effect of the mobile phase apparent pH on the retention and enantioseparation of *N*-derivatized amino acids. Conditions: mobile phase, ACN/0.1 M ammonium acetate (80/20, v/v) adjusted to different apparent pH values; other conditions as in **Table 3**.

Table 5. Effect of the buffer concentration on the retention and enantioseparation of *N*-derivatized amino acids. Conditions: ACN/different concentrations of ammonium acetate (80/20, v/v) (apparent pH = 5.3); other conditions as in **Table 3**.

Table 6. Enantioseparation of *N*-derivatized amino acids. Conditions: mobile phase, [a]ACN/0.1 M ammonium acetate solution (80/20, v/v) (apparent pH = 5.3); [b] ACN/0.1 M ammonium acetate (50/50, v/v) (apparent pH = 5.3); [c] ACN/ 0.1 M ammonium acetate (40/60, v/v) (apparent pH = 5.3); other conditions as in **Fig. 3**; "/": the number of theoretical plates cannot be calculated.

Table 7. Comparison of retention factors, selectivity and enantioresolution for different *N*-derivatized leucine derivatives. Conditions as in **Fig. 3**.

Highlights

- A carbamoylated quinidine based monolith was prepared for using in micro-HPLC.
- This monolithic column exhibited great properties for chromatographic performance in micro-HPLC .
- A wide range of *N*-derivatized amino acids were systematically evaluated and successfully enantioresolved.

Figure 1a

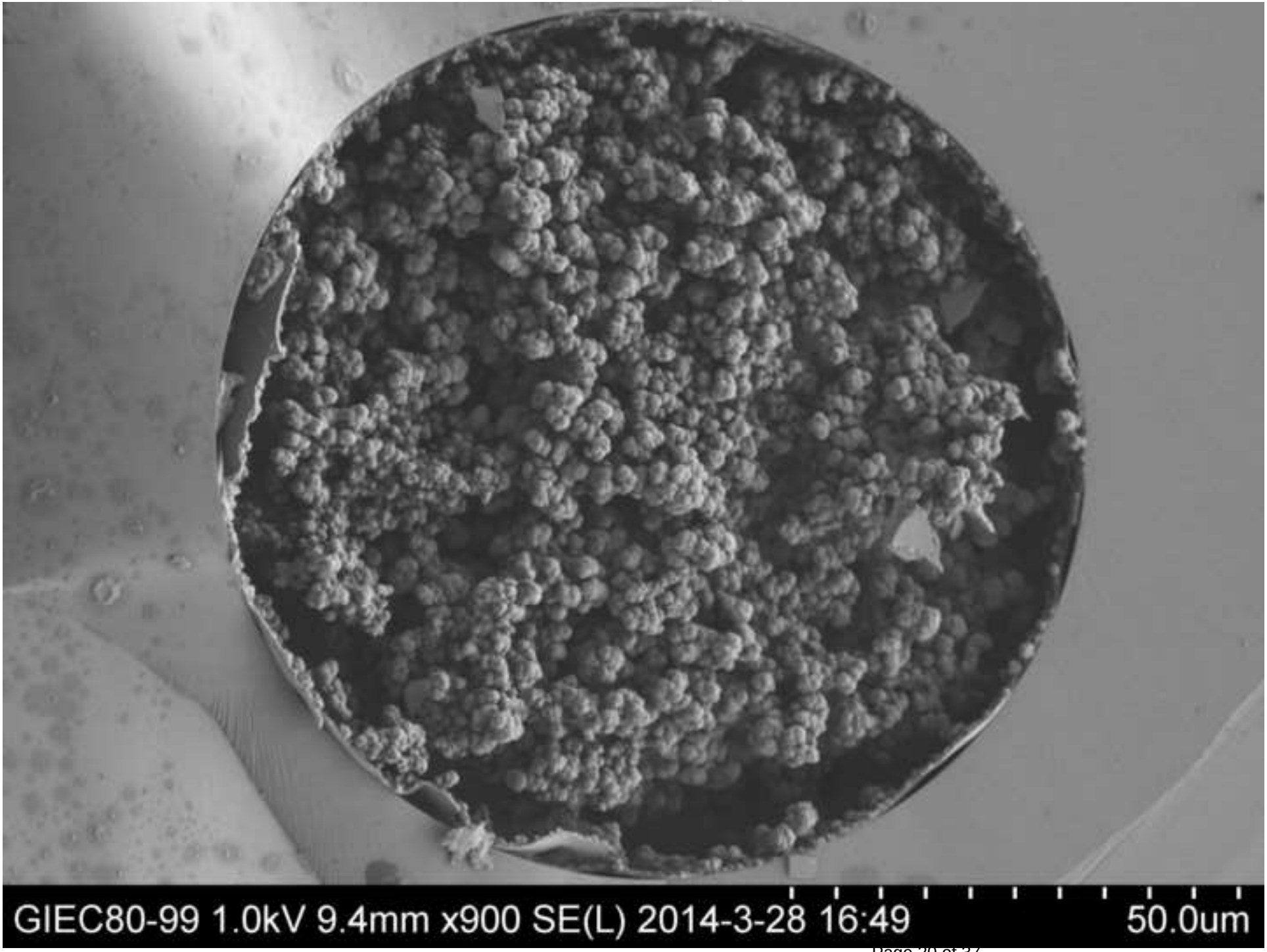

Figure 1b

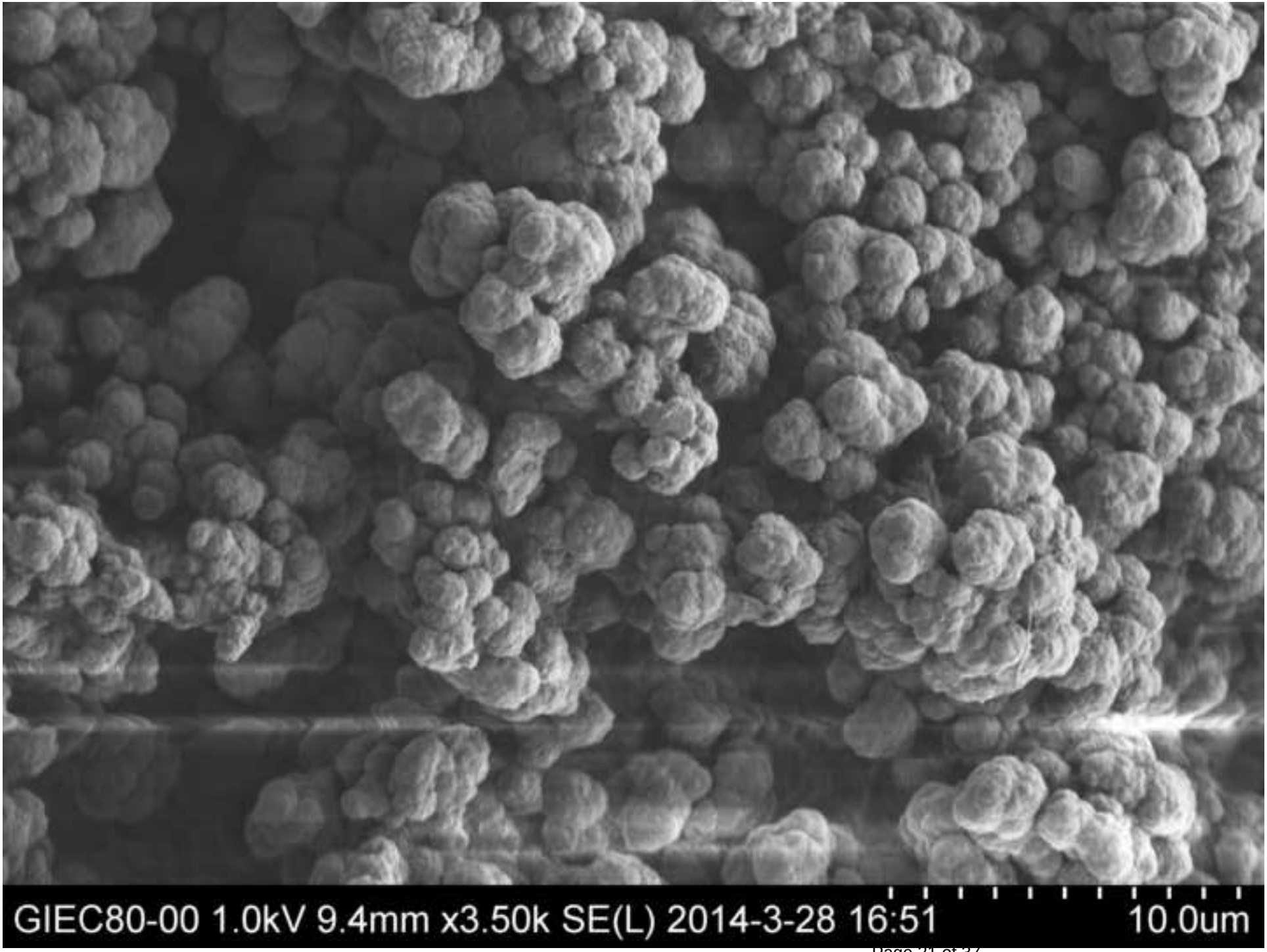

Fig. 2

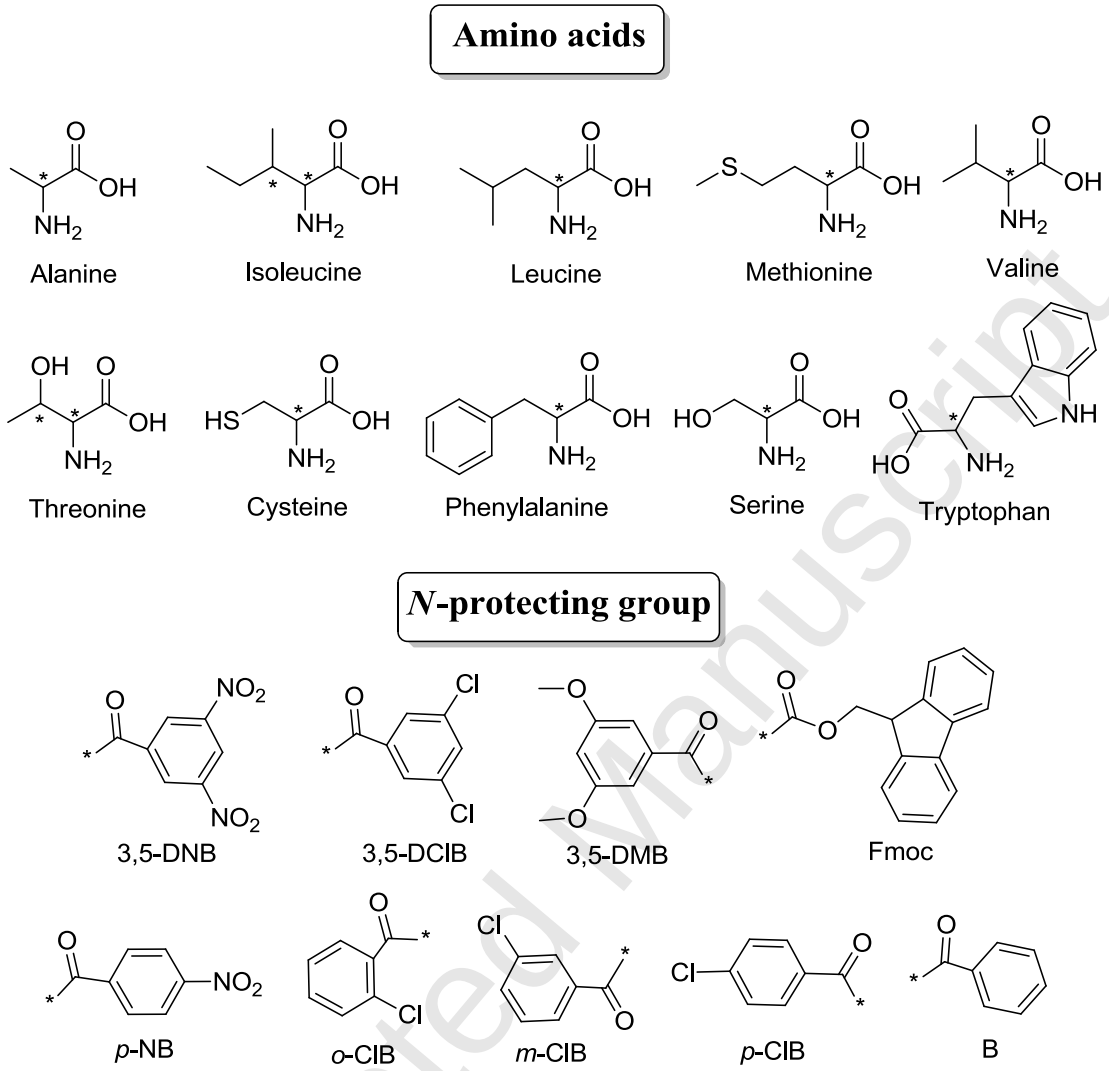

Fig. 3

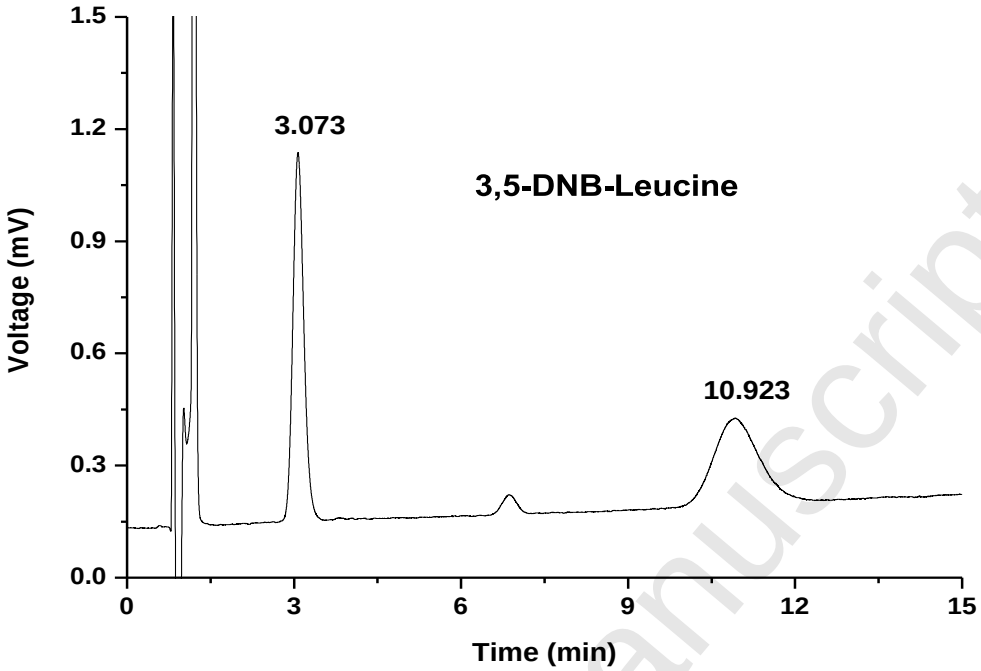

a

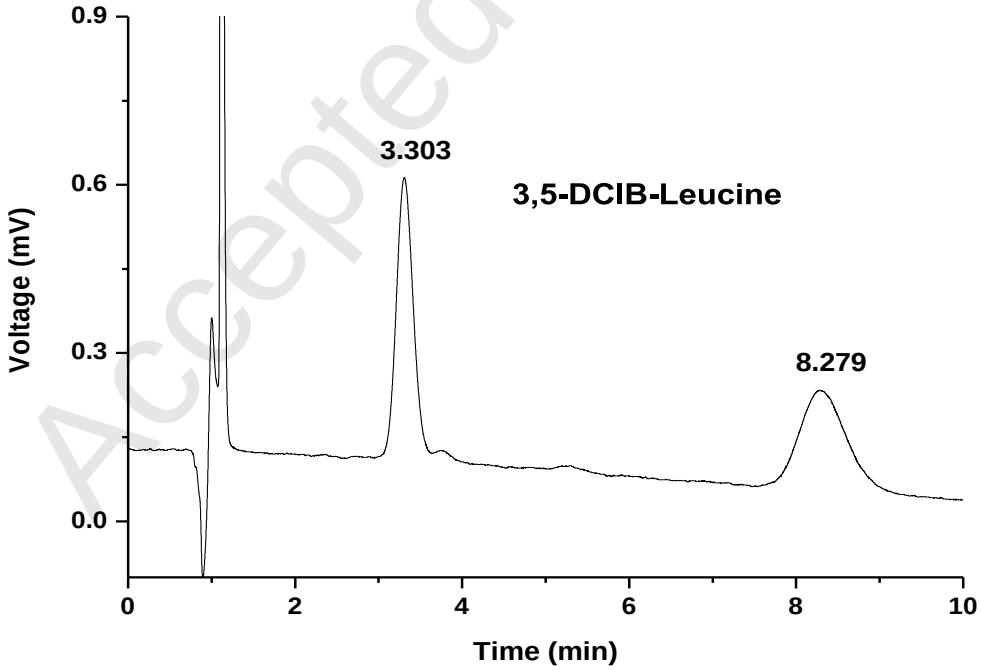

b

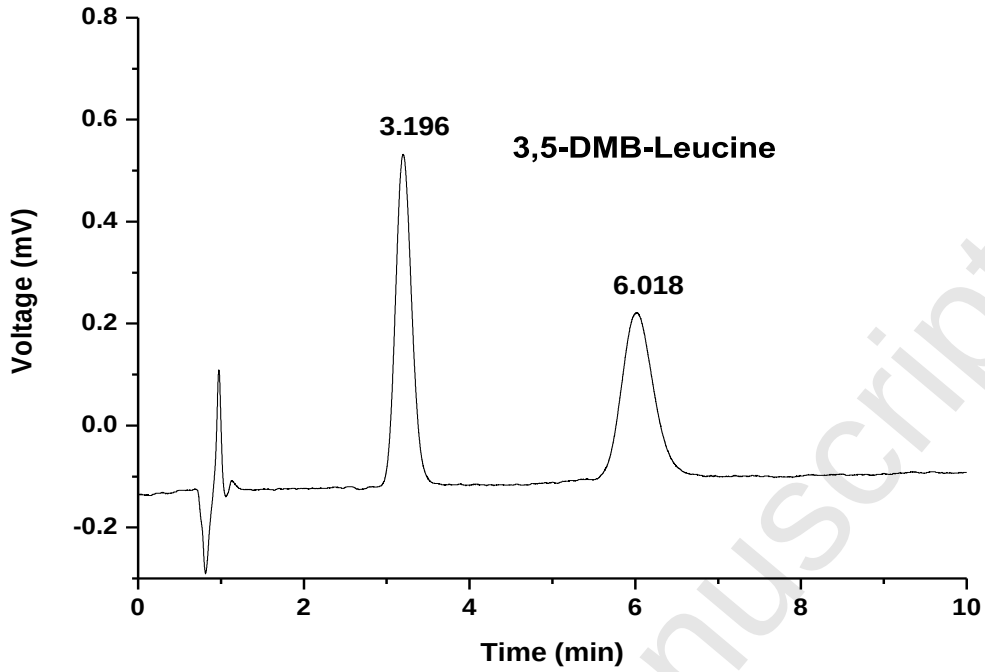

c

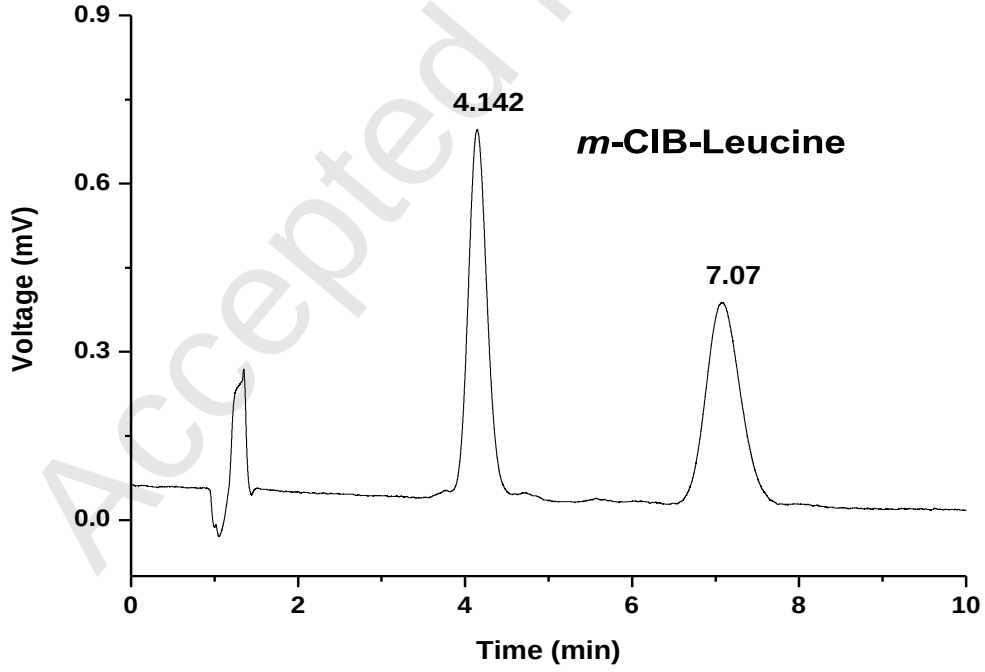

d

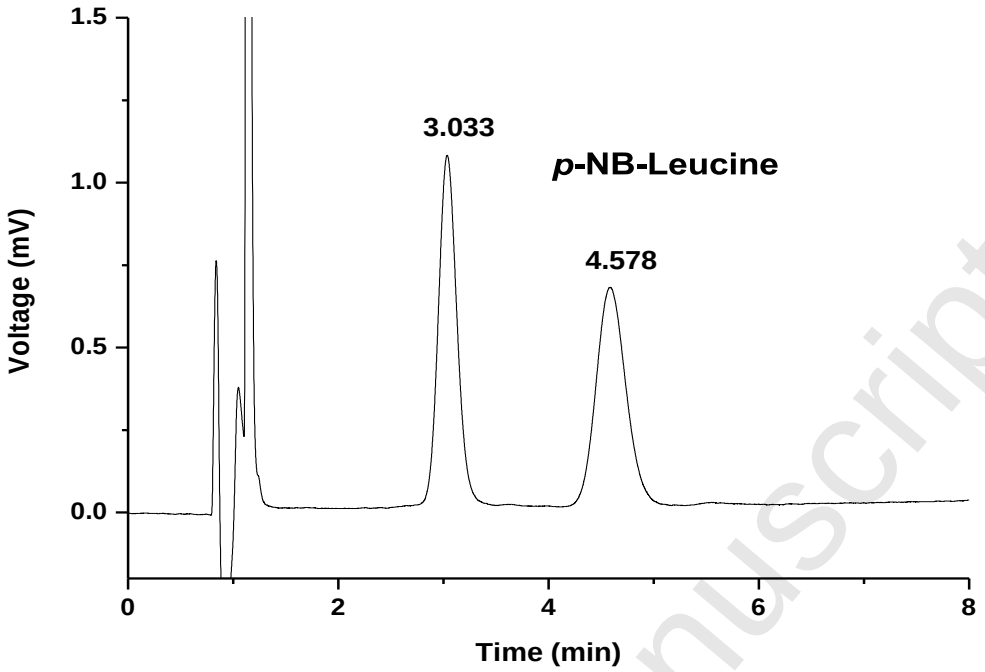

e

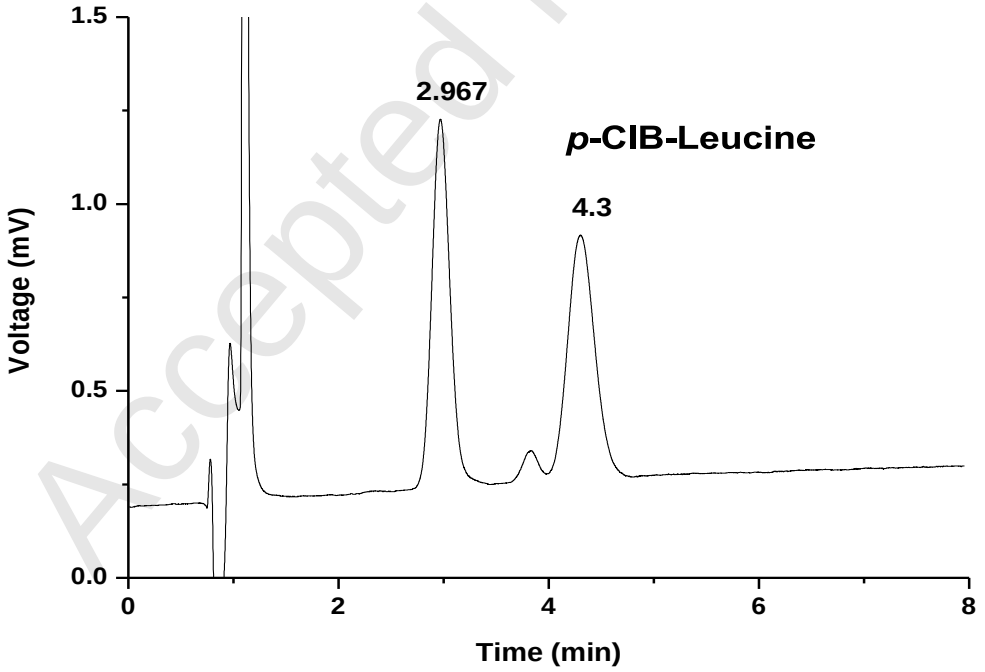

f

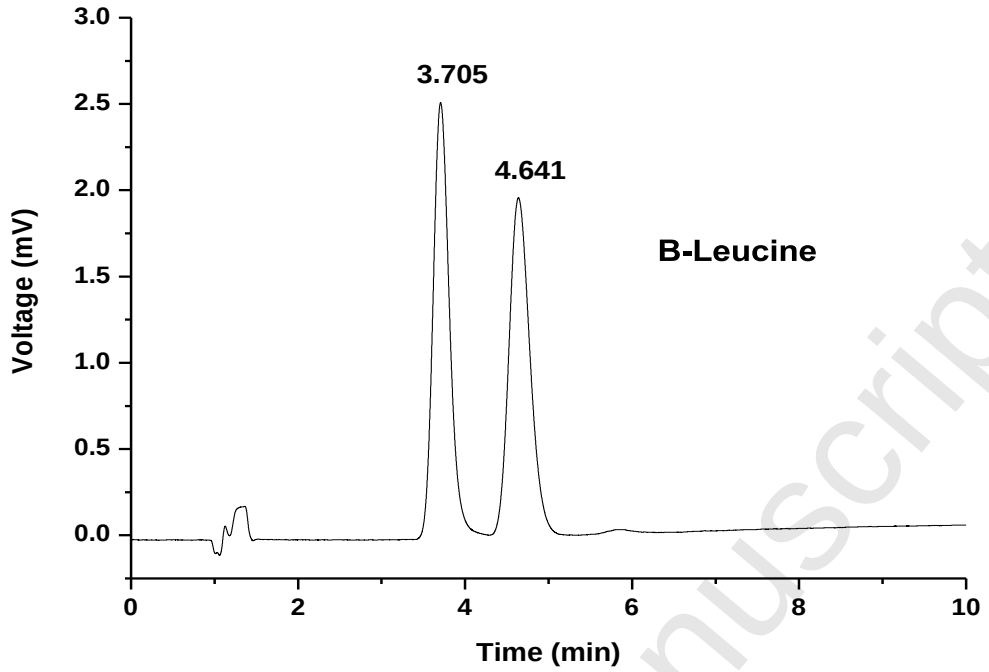

g

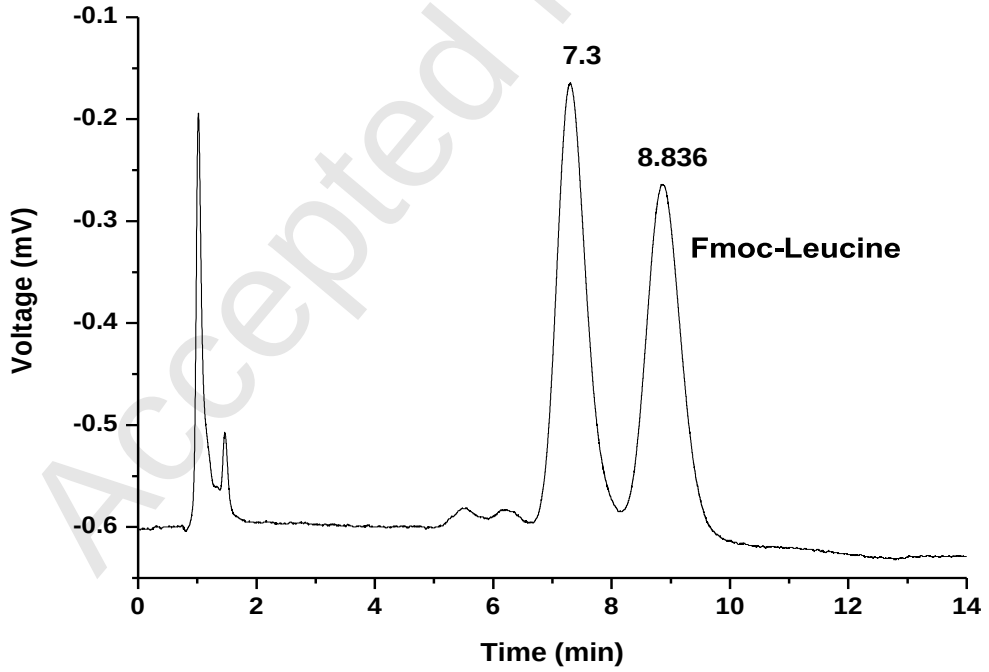

h

Fig. 4

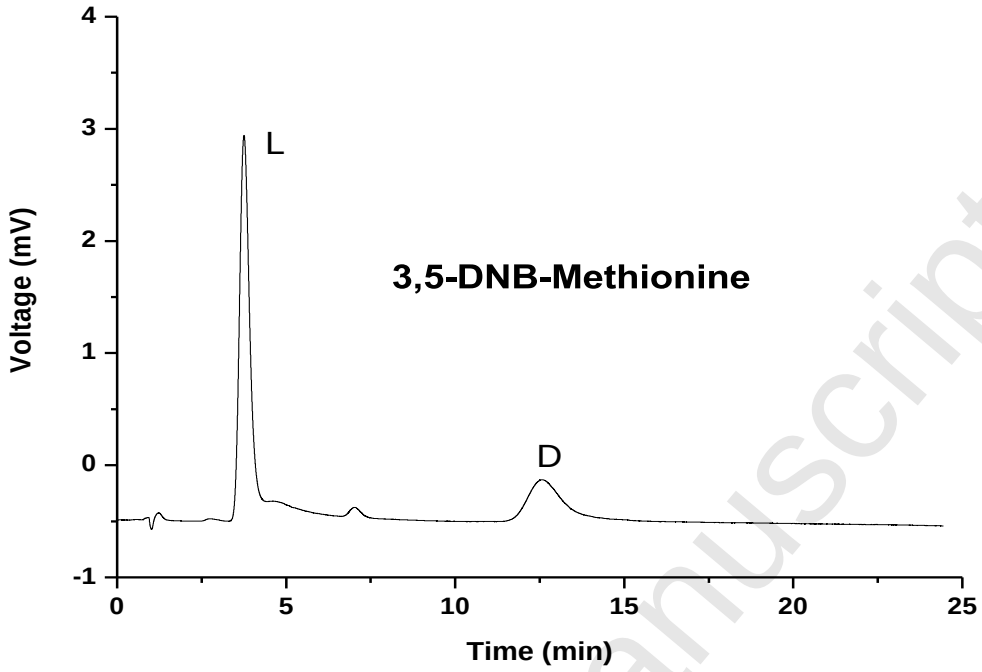

a

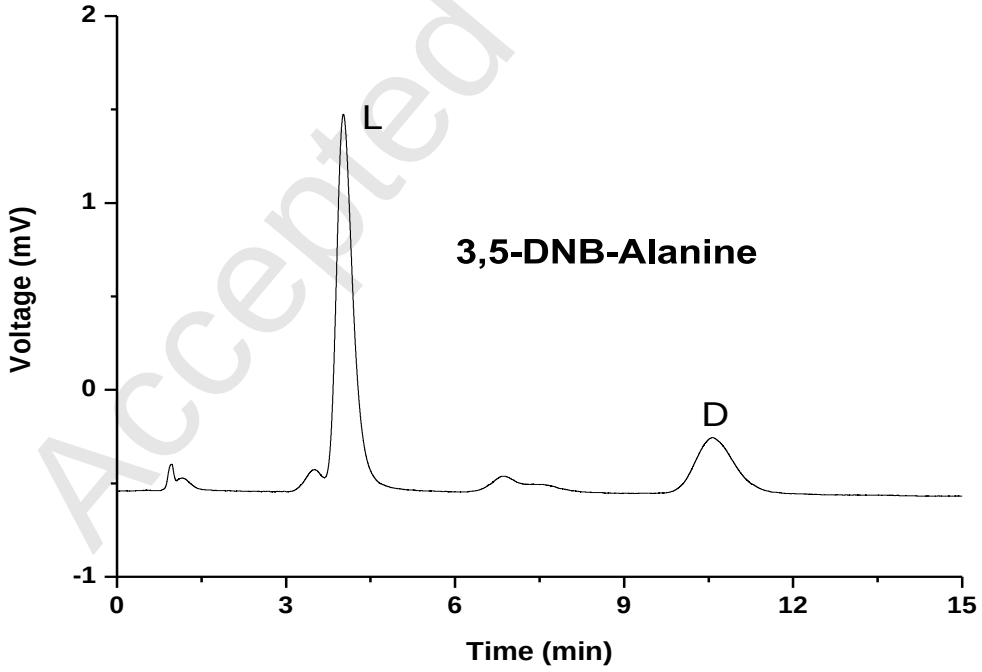

b

Fig. 5

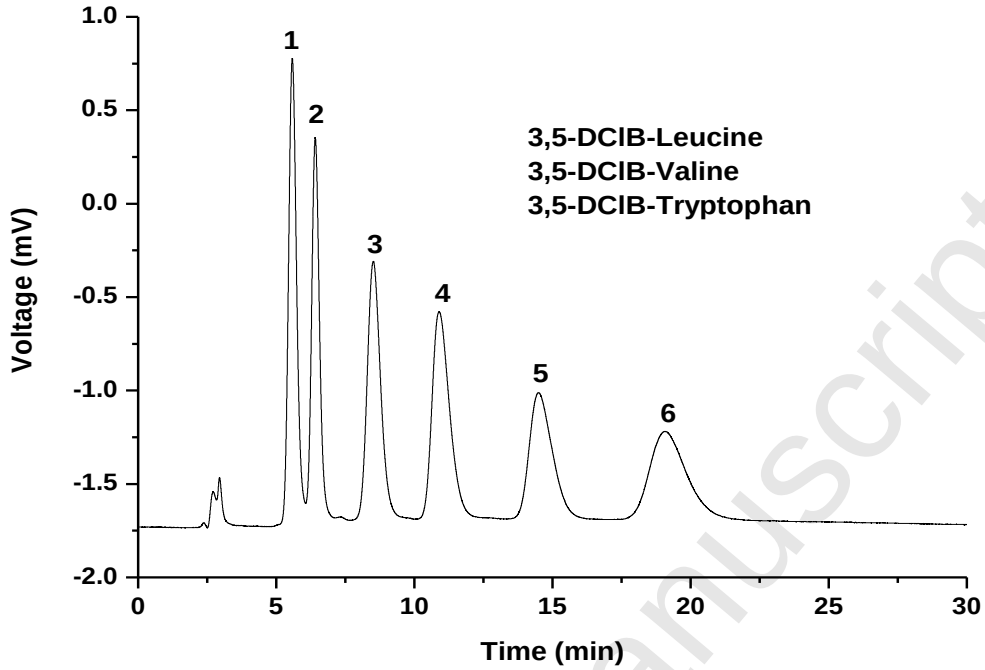

Table 1. Composition of the polymerization mixtures used for the preparation of poly(MQD-*co*-HEMA-*co*-EDMA) monolithic columns and their properties.

Column	Monomers (%, w/w)			Porogens (%,w/w)		Monomers : Porogens (%, w/w)		Back-pressure (MPa)	Theoretical plates (m^{-1})
	MQD	HEMA	EDMA	Dodecanol	Cyclohexanol				
C1	20	52.5	27.5	83.33	16.67	30	70	2.9	20600
C2	20	52.5	27.5	83.33	16.67	35	65	5.4	24400
C3	20	52.5	27.5	83.33	16.67	40	60	10.1	21000
C4	20	55	25	83.33	16.67	35	65	5.6	26500
C5	20	57.5	22.5	83.33	16.67	35	65	6.2	32000
C6	20	60.0	20.0	83.33	16.67	35	65	19.2	26200
C7	20	57.5	22.5	88.33	11.67	35	65	5.8	20500
C8	20	57.5	22.5	78.33	21.67	35	65	13.1	20700

Conditions: column dimensions: 150 mm × 100 μm I.D.; mobile phase, ACN/H_2O (40/60, v/v); UV detection wavelength: 214 nm; flow rate: 1 μL/min; injection volume: 20 nL; sample: naphthalene.

Table 2. Permeability of the poly(MQD-*co*-HEMA-*co*-EDMA) monolithic column

Mobile phase	**Relative polarity[a]**	**Viscosity η ($\times 10^{-3}$ Pa·s)[32]**	**Permeability K ($\times 10^{-13}$ m^2)**
ACN	0.460	0.369	1.547
MeOH	0.762	0.544	1.024
Water	1	0.890	0.839

[a] Relative polarity data were obtained from http://virtual.yosemite.cc.ca.us/smurov/orgsoltab.htm; viscosity data of pure solvents were obtained from reference [32].

Table 3. Effect of ACN content in the mobile phase on the retention and enantioseparation of *N*-derivatized amino acids.

	80%						70%						60%					
	k_1	k_2	α	R_s	N_1/m	N_2/m	k_1	k_2	α	R_s	N_1/m	N_2/m	k_1	k_2	α	R_s	N_1/m	N_2/m
3,5-DNB-Leucine	1.00	4.71	4.71	8.51	16600	8600	1.71	7.70	4.52	9.60	15400	9662	2.56	11.97	4.67	11.40	19400	11700
3,5-DClB-Leucine	1.01	3.15	3.12	6.64	16100	10200	1.88	5.67	3.03	8.04	15100	12377	2.94	9.16	3.11	9.69	20200	14100

Conditions: column: 150 mm × 100 μm I.D. poly(MQD-*co*-HEMA-*co*-EDMA); mobile phase: mixture of ACN and 0.1 M ammonium acetate at various ratios (apparent pH = 5.3); UV detection wavelength: 254 nm; flow rate: 1 μL/min; injection volume: 20 nL.

Table 7. Comparison of retention factor, selectivity and enantioresolution of different *N*-derivatized leucine derivatives.

Analyte	k_1	k_2	α	*Rs*
3,5-DNB-Leucine	1.00	4.71	4.71	8.51
3,5-DClB-Leucine	1.01	3.15	3.12	6.64
3,5-DMB-Leucine	2.35	5.31	2.26	5.30
m-ClB-Leucine	3.35	6.42	1.92	4.94
p-NB-Leucine	2.18	3.80	1.74	3.68
p-ClB-Leucine	2.11	3.51	1.66	3.34
B-Leucine	2.89	3.87	1.34	2.31
Fmoc-Leucine	6.66	8.27	1.24	1.53

Conditions as in **Fig. 3**.

Table 4. Effect of the mobile phase apparent pH on the retention and enantioseparation of *N*-derivatized amino acids.

	pH 6.3						pH 5.3						pH 4.3					
	k_1	k_2	α	R_s	N_1/m	N_2/m	k_1	k_2	α	R_s	N_1/m	N_2/m	k_1	k_2	α	R_s	N_1/m	N_2/m
3,5-DNB-Leucine	2.26	10.55	4.68	10.52	14600	10600	1.00	4.71	4.71	8.51	16600	8600	0.48	1.91	3.96	4.36	7200	5200
3,5-DClB-Leucine	4.60	14.22	3.09	8.80	12200	11500	1.01	3.15	3.12	6.64	16100	10200	0.49	1.25	2.55	3.01	8100	6400

Conditions: mobile phase, ACN/0.1 M ammonium acetate (80/20, v/v) adjusted to different apparent pH values; other conditions as in **Table 3**.

Table 5. Effect of the buffer concentration on the retention and enantioseparation of *N*-derivatized amino acids.

	0.15 M						0.10 M						0.05 M					
	k_1	k_2	α	R_s	N_1/m	N_2/m	k_1	k_2	α	R_s	N_1/m	N_2/m	k_1	k_2	α	R_s	N_1/m	N_2/m
3,5-DNB-Leucine	0.77	3.63	4.70	7.75	13600	8600	1.00	4.71	4.71	8.51	16600	8600	1.71	7.88	4.61	10.38	15000	11500
3,5-DClB-Leucine	0.73	2.36	3.22	6.05	14000	10500	1.01	3.15	3.12	6.64	16100	10200	1.70	5.40	3.18	7.94	17900	10600

Conditions: ACN/different concentrations of ammonium acetate (80/20, v/v) (apparent pH = 5.3); other conditions as in **Table 3**.

Table 6. Enantioseparation of *N*-derivatized amino acids.

Sapmle	k_1	k_2	α	*Rs*	N_1/m	N_2/m
3,5-DNB-Isoleucine[a]	2.56	17.88	6.98	8.74	4500	4200
3,5-DNB-Valine[a]	2.93	16.26	5.55	8.92	7400	5000
3,5-DNB-Tryptophan[a]	4.43	22.00	4.97	7.32	4400	3600
3,5-DNB-Leucine[a]	1.00	4.71	4.71	8.51	16600	8600
3,5-DNB-Phenyalanine[a]	3.27	15.21	4.65	9.95	4900	4200
3,5-DNB-Methionine[a]	3.05	13.24	4.33	8.09	8400	5100
3,5-DNB-Threonine[a]	3.86	14.07	3.64	8.14	6000	6700
3,5-DNB-Cysteine[a]	5.68	19.88	3.50	4.31	2000	1900
3,5-DNB-Alanine[a]	3.55	11.30	3.19	8.06	10700	7400
3,5-DNB-Serine[a]	4.52	14.05	3.11	8.47	10500	8400
3,5-DClB-Isoleucine[a]	1.31	5.58	4.24	8.71	17100	9200
3,5-DClB-Valine[a]	1.39	4.76	3.42	8.74	19200	12800
3,5-DClB-Phenyalanine[a]	2.29	7.65	3.33	8.17	15400	9400
3,5-DClB-Leucine[a]	1.01	3.15	3.12	6.64	16100	10200
3,5-DClB-Tryptophan[a]	2.33	7.13	3.06	6.87	10400	8000
3,5-DClB-Methionine[a]	1.39	4.10	2.95	7.33	13300	13100
3,5-DClB-Threonine[a]	2.15	5.52	2.57	8.00	21000	15400
3,5-DClB-Cystenine[a]	3.41	7.78	2.28	5.22	14000	6300
3,5-DClB-Alanine[a]	1.94	4.30	2.21	6.79	22100	16300
3,5-DClB-Serine[a]	2.70	5.88	2.18	7.55	23800	18800
Fmoc-Isoleucine[b]	9.58	13.50	1.41	2.90	9700	8800
Fmoc-Valine[b]	8.20	11.47	1.40	2.76	9100	8600

Fmoc-Phenylalanine[b]	9.33	11.82	1.27	1.84	7800	7600
Fmoc-Cysteine[c]	13.91	17.61	1.27	1.58	5500	5400
Fmoc-Tryprophan[b]	12.18	15.33	1.26	1.69	7100	6300
Fmoc-Leucine[b]	6.66	8.27	1.24	1.53	6900	6900
Fmoc-Serine[b]	4.43	5.47	1.23	1.56	9100	8300
Fmoc-Methionine[b]	5.82	7.08	1.22	1.43	7700	7500
Fmoc-Alanine[c]	8.40	9.77	1.16	1.38	10100	9900
3,5-DMB-Leucine[a]	2.35	5.31	2.26	5.30	8300	7800
3,5-DMB-Methionine[a]	2.12	4.20	1.98	4.50	9500	8100
3,5-DMB-Alanine[a]	2.06	3.53	1.71	3.98	12700	10300
p-NB-Leucine[a]	2.18	3.80	1.74	3.68	9400	8300
p-NB-Methionine[a]	2.74	4.43	1.62	3.75	11500	10500
p-NB-Threonine[a]	3.93	5.87	1.49	3.91	15500	14700
p-NB-Alanine[a]	2.69	3.84	1.43	3.08	14100	13800
m-ClB-Leucine[a]	3.35	6.42	1.92	4.94	11000	8800
m-ClB-Threonine[a]	3.44	5.72	1.67	4.43	12600	12600
m-ClB-Alanine[a]	3.08	4.67	1.52	3.72	14200	13400
m-ClB-Methionine[a]	2.83	3.70	1.31	2.22	12800	12400
p-ClB-Leucine[a]	2.11	3.51	1.66	3.34	9400	8400
p-ClB-Methionine[a]	3.03	4.62	1.52	3.53	12600	11900
p-ClB-Alanine[a]	2.95	4.02	1.36	2.87	16100	14700
B-Leucine[a]	2.89	3.87	1.34	2.31	11800	10900
B-Methionine[a]	2.81	3.67	1.31	2.17	12500	11700
B-Threonine[a]	4.25	5.32	1.25	2.27	16400	15500

o-ClB-Methionine[a]	5.83	6.30	1.08	0.74	/	/

Conditions: mobile phase, [a]ACN/0.1 M ammonium acetate solution (80/20, v/v) (apparent pH = 5.3); [b] ACN/0.1 M ammonium acetate (50/50, v/v) (apparent pH = 5.3); [c] ACN/ 0.1 M ammonium acetate (40/60, v/v) (apparent pH = 5.3); other conditions as in **Fig. 3**; "/": the number of theoretical plates cannot be calculated.